

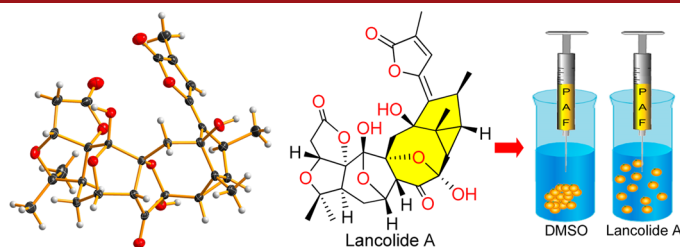
Lancolides, Antiplatelet Aggregation Nortriterpenoids with Tricyclo[6.3.0.0^{2,11}]undecane-Bridged System from *Schisandra lancifolia*

Yi-Ming Shi,^{†,§,⊥} Xin-Bo Wang,^{†,⊥} Xiao-Nian Li,[†] Xiao Luo,[†] Zi-Ying Shen,[‡] Yi-Ping Wang,^{*,‡} Wei-Lie Xiao,^{*,†} and Han-Dong Sun^{*,†}

State Key Laboratory of Phytochemistry and Plant Resources in West China, Kunming Institute of Botany, Chinese Academy of Sciences, Kunming 650201, Yunnan, P. R. China, Shanghai Institute of Materia Medica, Chinese Academy of Sciences, Shanghai 201203, P. R. China, and University of Chinese Academy of Sciences, Beijing 100049, P. R. China
ypwang@mail.shnc.ac.cn; xwl@mail.kib.ac.cn; hdsun@mail.kib.ac.cn

Received August 21, 2013

ABSTRACT



A new class of highly oxygenated *Schisandra* nortriterpenoids, lancolides A–D (1–4), from *Schisandra lancifolia*, represents the first example of natural products that possess a tricyclo[6.3.0.0^{2,11}]undecane-bridged system. Their structures were elucidated by NMR spectra, X-ray diffraction, and quantum chemical calculations. Lancolides A (1) and D (4) had specific antiplatelet aggregation induced by platelet-activating factor (PAF).

Schisandra nortriterpenoids (SNTs), which are characterized by highly oxygenated polycyclic ring systems, are structurally diverse and exquisitely complicated natural products from plants of *Schisandra* genus.¹ Sixteen

fascinating skeletons of these secondary metabolites have hitherto been discovered through considerable endeavors in phytochemically systematic research.^{1,2} Recently, new light has been shed onto the area of synthetic^{1,3} and quantum chemical⁴ research of SNTs, and therefore, the formidable polycyclic skeletons have led to the development of some chemical reactions and strategies that have

[†] Kunming Institute of Botany.

[§] University of Chinese Academy of Sciences.

[‡] Shanghai Institute of Materia Medica.

[⊥] These authors contributed equally.

(1) Xiao, W. L.; Li, R. T.; Huang, S. X.; Pu, J. X.; Sun, H. D. *Nat. Prod. Rep.* **2008**, *25*, 871–891.

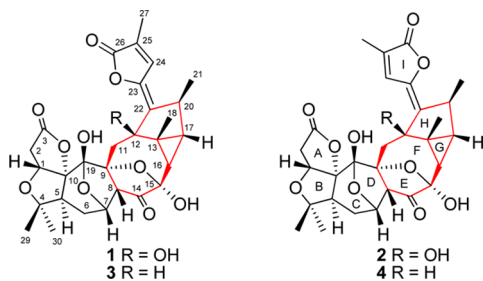
(2) (a) Lo, I. W.; Lin, Y. C.; Liao, T. C.; Chen, S. Y.; Lin, P. H.; Chien, C. T.; Chang, S. Y.; Shen, Y. C. *Food Chem.* **2013**, *136*, 1095–1099. (b) Luo, X.; Shi, Y. M.; Luo, R. H.; Luo, S. H.; Li, X. N.; Wang, R. R.; Li, S. H.; Zheng, Y. T.; Du, X.; Xiao, W. L.; Pu, J. X.; Sun, H. D. *Org. Lett.* **2012**, *14*, 1286–1289. (c) Wang, J. R.; Kurtán, T.; Mándi, A.; Guo, Y. W. *Eur. J. Org. Chem.* **2012**, 5471–5482. (d) Shi, Y. M.; Li, X. Y.; Li, X. N.; Luo, X.; Xue, Y. B.; Liang, C. Q.; Zou, J.; Kong, L. M.; Li, Y.; Pu, J. X.; Xiao, W. L.; Sun, H. D. *Org. Lett.* **2011**, *13*, 3848–3851. (e) Lin, Y. C.; Lo, I. W.; Chen, S. Y.; Lin, P. H.; Chien, C. T.; Chang, S. Y.; Shen, Y. C. *Org. Lett.* **2011**, *13*, 446–449. (f) Cheng, Y. B.; Liao, T. C.; Lo, I. W.; Chen, Y. C.; Kuo, Y. C.; Chen, S. Y.; Chien, C. T.; Shen, Y. C. *Org. Lett.* **2010**, *12*, 1016–1019. (g) Luo, X.; Chang, Y.; Zhang, X. J.; Pu, J. X.; Gao, X. M.; Wu, Y. L.; Wang, R. R.; Xiao, W. L.; Zheng, Y. T.; Lu, Y.; Chen, G. Q.; Zheng, Q. T.; Sun, H. D. *Tetrahedron Lett.* **2009**, *50*, 5962–5964.

(3) (a) Ren, W. W.; Chen, Z. X.; Xiao, Q.; Li, Y.; Sun, T. W.; Zhang, Z. Y.; Ye, Q. D.; Meng, F. K.; You, L.; Zhao, M. Z.; Xu, L. M.; Tang, Y. F.; Chen, J. H.; Yang, Z. *Chem.—Asian J.* **2012**, *7*, 2341–2350 and the preceding two papers in this issue. (b) Goh, S. S.; Baars, H.; Gockel, B.; Anderson, E. A. *Org. Lett.* **2012**, *14*, 6278–6281. (c) Bartoli, A.; Chouraqui, G.; Parrain, J. L. *Org. Lett.* **2012**, *14*, 122–125. (d) Xiao, Q.; Ren, W. W.; Chen, Z. X.; Sun, T. W.; Li, Y.; Ye, Q. D.; Gong, J. X.; Meng, F. K.; You, L.; Liu, Y. F.; Zhao, M. Z.; Xu, L. M.; Shan, Z. H.; Shi, Y.; Tang, Y. F.; Chen, J. H.; Yang, Z. *Angew. Chem., Int. Ed.* **2011**, *50*, 7373–7377. (e) Maity, S.; Matcha, K.; Ghosh, S. J. *Org. Chem.* **2010**, *75*, 4192–4200. (f) Cordonnier, M. C. A.; Kan, S. B. J.; Anderson, E. A. *Chem. Commun.* **2008**, 5818–5820.

(4) (a) Xiao, W. L.; Lei, C.; Ren, J.; Liao, T. G.; Pu, J. X.; Pittman, C. U.; Lu, Y.; Zheng, Y. T.; Zhu, H. J.; Sun, H. D. *Chem.—Eur. J.* **2008**, *14*, 11584–11592. (b) Chenoweth, D. M.; Chenoweth, K.; Goddard, W. A. *J. Org. Chem.* **2008**, *73*, 6853–6856.

culminated in the accomplishment of the total synthesis of schindilactone A for the first time.^{3d}

Schisandra lancifolia (Rehd. et Wils.) A. C. Smith, a species of the *Schisandra* genus of the family Schisandraceae endemic to the southwest China, could be regarded as a prolific source of SNTs.^{1,2b,2g} Previous chemical research on *S. lancifolia* collected in the Nujiang prefecture of Yunnan province in China led to the discovery of five unique SNTs,^{2b,g} which were quite different from those isolated from this species collected in the Dali prefecture of Yunnan province.¹ This might be generated by the different ecological environment, resulting in a change in expression of the enzymes related to the cyclization and oxidation of squalene. Motivated by the intriguing architectures, the plant was recollected and some particular fractions were subjected to meticulous chemical study. Interestingly, after several steps of separation, the RP-HPLC profiles displayed four peaks with an unusual maximum UV absorption band at 300 nm (Figure S1, Supporting Information) that was 25 nm red-shifted in comparison to the maximum UV absorption bands of schilancitrilactones A–C^{2b} and schilancidilactones A and B.^{2g} This phenomenon allowed us to preliminarily propose these four components featuring chromophores which are a little different from those of the reported compounds. Finally, these four compounds, lancolides A–D (**1–4**), were successfully purified according to the procedure described in the Supporting Information.



The molecular formula of **1** was determined as C₂₉H₃₂O₁₁ by positive ESIMS and HREIMS (*m/z* 556.1954), requiring 14 degrees of unsaturation. The ¹³C NMR and DEPT spectra exhibited 29 carbon resonances, including seven sp² carbon signals that were ascribed to one carbonyl group (δ_C 210.6), two ester groups (δ_C 170.6 and 176.9), and two double bonds (δ_C 128.4, 137.2, 139.3, and 142.7). These sp² carbon signals accounted for five of 14 degrees of unsaturation

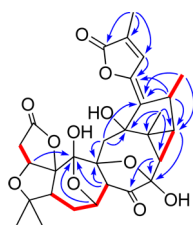


Figure 1. Selected HMBC (from H to C, arrow in blue) and ¹H–¹H COSY (dash in red) correlations of **1**.

and thus indicated **1** must be a polycyclic compound. Carbon resonances for additional five methyls, three methylenes, seven methines (of which two are oxygenated), and seven quaternary carbons (of which six are oxygenated) were observed. This evidence implied that **1** was a highly oxygenated condensed SNT. Comparison of the 1D NMR data of **1** (Tables S1 and S2, Supporting Information) with those of schilancitrilactone A evidently suggested similar substructures of rings A, B, and I for both compounds.^{2b} The residue structure could be elucidated on the basis of 2D NMR spectra (Figure 1). Analysis of the ¹H–¹H COSY spectrum starting from the proton signal at δ_H 2.47 (H-5) revealed the presence of a spin system of H-5/H₂-6/H-7/H-8. Coupling with the HMBC correlations of H-8 (δ_H 3.66) with C-9 (δ_C 85.1) and of H-1 (δ_H 4.84) and H-8 with a hemiketal carbon (δ_C 105.3) suggested the existence of a highly oxygenated seven-membered carbon ring fused with ring B. The key HMBC correlation of an oxymethine (H-7, δ_H 4.57) with C-19 indicated a unique oxa-bridged hemiketal lay within the seven-membered carbon ring. The characteristic signals of C-9 (δ_C 85.1), C-14 (δ_C 210.6), and C-15 (δ_C 106.1) for ring E could be obviously distinguished.^{2c} Ring F was established on the basis of the HMBC correlations of H₂-11 (δ_H 2.15 and 3.96) with C-9 and C-12 (δ_C 81.0), of H-16 (δ_H 0.92) with C-14 and C-15, and of Me-18 (δ_H 1.32) with C-12, C-13 (δ_C 37.2), and C-16 (δ_C 33.8). A three-membered carbon ring (ring G) containing C-13, C-16 (δ_C 33.8 and δ_H 0.92), and C-17 (δ_C 36.2 and δ_H 1.34) was deduced from the characteristic signals in high-field region of the 1D NMR data and was further supported by the HMBC correlation of Me-18 with C-17 and the ¹H–¹H COSY correlation of H-16 with H-17. Although the ¹H–¹H COSY correlation between H-17 and H-20 (δ_H 3.36) was not observed, the HMBC correlation of H-20 with C-17 gave rise to the connectivity of C-17 and C-20 (δ_C 34.9). In addition, H₂-11, H-20, and Me-21 (δ_H 1.37) signals simultaneously showed HMBC correlations with an olefinic carbon signal (δ_C 139.3). This evidence suggested the presence of a five-membered-carbon ring (ring H) containing C-12, C-13, C-17, C-20, and C-22. Thus, an unprecedented tricyclo[6.3.0.0^{2,11}]undecane-bridged system was established, which was formed by an eight-, a three-, and a five-membered rings. The connection between ring I and H through a carbon–carbon double bond was supported by

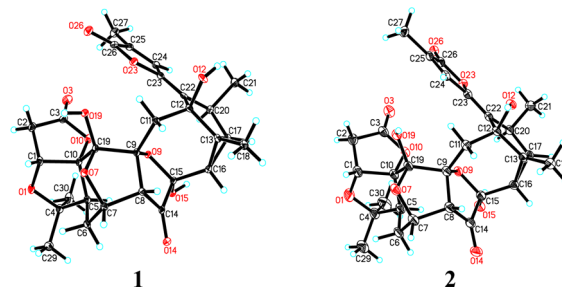


Figure 2. X-ray crystallographic structures of **1** and **2**.

the HMBC correlation of H-20 with C-23. The double bond of C-22/C-23 was assigned to be *Z* geometry based on the ROESY correlations of H-24 with H-20 and Me-21.

Compound **1** was recrystallized in methanol to afford colorless block crystals of the orthorhombic space group *P*212121. The X-ray diffraction analysis was applied to confirm the novel carbon skeleton, which resulted in a Flack parameter of 0.16(13) (CCDC 948232) (Figure 2). On the basis of the relative configuration demonstrated by the X-ray diffraction, the quantum chemical calculation study for electronic circular dichroism (ECD) was conducted to determine its absolute configuration using time-dependent density-functional theory (TDDFT) method.⁵ Consequently, we needed to calculate the structures for a pair of enantiomers, (1*R*,5*S*,7*S*,8*R*,9*R*,10*R*,12*R*,13*R*,15*S*,16*S*,17*R*,19*S*,20*S*)-**1** and (1*S*,5*R*,7*R*,8*S*,9*S*,10*S*,12*S*,13*S*,15*R*,16*R*,17*S*,19*R*,20*R*)-**1**. As illustrated in Figure 3, the experimental ECD spectrum of **1** was consistent with the ECD curve calculated for (1*R*,5*S*,7*S*,8*R*,9*R*,10*R*,12*R*,13*R*,15*S*,16*S*,17*R*,19*S*,20*S*)-**1**.

Molecular orbital (MO) analysis of the single conformer **1a** afforded exact comprehension of the experimental ECD curve (Figure 4). The electronic transitions from MO146 to MO149 involving an $n \rightarrow \pi^*$ transition of the carbonyl group in the eight-membered carbon ring afforded the positive rotatory strength at 321 nm, which could be ascribed to the experimental positive Cotton effect (CE) at 323 nm. The electronic transitions from MO147 to MO148 involving a $\pi \rightarrow \pi^*$ transition of the $\alpha,\beta,\gamma,\delta$ -unsaturated γ -lactone played a dominant role to give rise to the negative rotatory strength at 311 nm, which could be assigned to the experimental negative CE at 301 nm. The positive rotatory strength at 253 nm could be assigned to the experimental positive CE at 265 nm. Accordingly, MO141 to MO148, the transitions from a pseudo- π -type MO generated by the three-membered carbon ring⁶ to a π^* -type MO, attributed to this absorption band. Another positive CE at 207 nm in the experimental curve correlated with the positive rotatory strength at 230 nm, which was contributed by the dominant electronic transitions from MO137 to MO148. Therefore, the absolute configuration of **1** was determined as shown.

The molecular formula of **2**, C₂₉H₃₂O₁₁, was determined by positive ESIMS and HREIMS. It was found that the NMR data of **1** and **2** (Tables S1 and S2, Supporting Information) were quite similar. Careful comparison of their NMR data indicated that the minor differences might result from the distinct geometry of C-22/C-23 double bond between **1** and **2**. Subsequent ROESY analysis of **2** revealed the C-22/C-23 double bond to be *E* geometry, which was judged by the ROESY correlation of H-24 (δ_{H} 7.58) with H-11 α (δ_{H} 3.58). Furthermore, its absolute configuration was assigned to be 1*R*,5*S*,7*S*,8*R*,9*R*,10*R*,12*R*,13*R*,15*S*,16*S*,17*R*,19*S*,20*S*, which was supported by X-ray diffraction (CCDC 948233) (Figure 2) and ECD calculation (Figure S2, Supporting Information).

(5) (a) Bringmann, G.; Bruhn, T.; Maksimenka, K.; Hemberger, Y. *Eur. J. Org. Chem.* **2009**, 2717–2727. (b) Berova, N.; Di Bari, L.; Pescitelli, G. *Chem. Soc. Rev.* **2007**, 36, 914–931.

(6) Garcia, A.; Elorza, J. M.; Ugalde, J. M. *Phys. Chem. Chem. Phys.* **1999**, 1, 2203–2207.

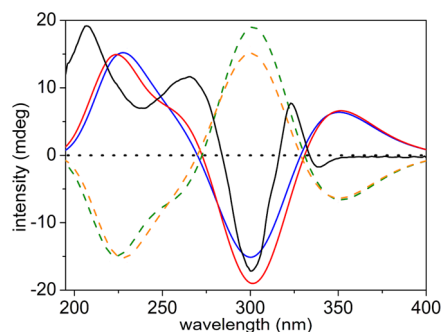


Figure 3. Experimental ECD of **1** (black), calculated ECD of **1** in the gas phase (blue) and in methanol (red), and calculated ECD of *ent*-**1** in the gas phase (orange) and in methanol (green).

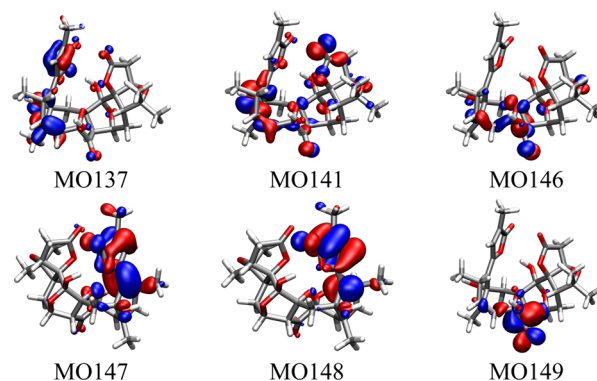


Figure 4. Important MOs in ECD of the optimized conformer **1a** at the B3LYP/6-31+G(d,p) level in methanol with PCM model.

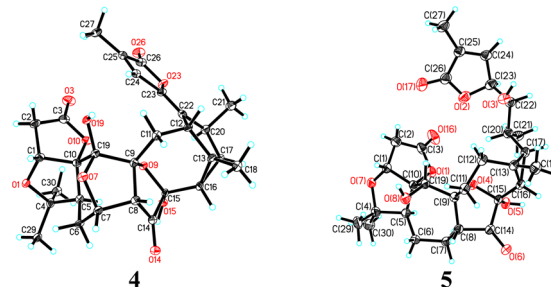


Figure 5. X-ray crystallographic structures of **4** and **5**.

Compounds **3** and **4** were identified to be 12-deoxy derivatives of **1** and **2**, respectively, which were supported by the MS data and HMBC and ¹H–¹H COSY correlations. On the basis of the relative configurations determined by their ROESY spectra, the absolute configuration of **3** was established by calculated ECD (Figure S3, Supporting Information), and that of **4** was determined

Scheme 1. Hypothetical Biogenetic Pathway of Lancolide A (1)

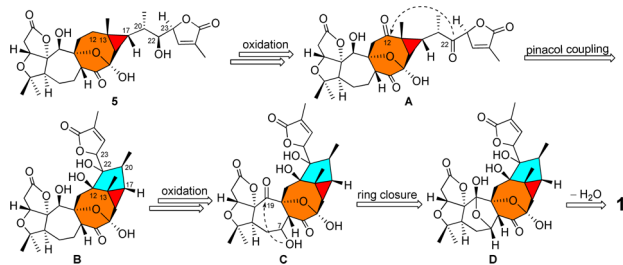


Table 1. Antiplatelet Aggregation Activity of Compounds 1–5.^a

compd	PAF	collagen	AA	thrombin
1	63.2 ± 1.7	2.2 ± 3.9	0.0 ± 0.0	0.0 ± 0.0
2	20.0 ± 5.3	1.0 ± 2.0	0.0 ± 0.0	15.3 ± 7.2
3	4.1 ± 5.8	3.8 ± 4.0	2.3 ± 4.0	27.5 ± 14.1
4	65.6 ± 1.1	17.7 ± 2.8	5.5 ± 7.7	27.5 ± 7.1
5	29.3 ± 1.0	5.9 ± 8.5	1.8 ± 3.1	0.0 ± 0.0

^aInhibition % ± SD at 100 μg/mL (SD = standard deviation).

by X-ray diffraction (CCDC 948234) (Figure 5) and ECD calculation (Figure S4, Supporting Information).

Compounds 1–4 represent a novel class of triterpenoids wherein they involve unique bridged systems. Two oxabridged hemiketals within the 7/8 fused carbocyclic ring and the 7/8/3/5 consecutive carbocyclic core make 1–4 represent the most complex members in the family of SNTs so far. Most notably, these new members can be recognized as the first example of natural products characterized with a tricyclo[6.3.0.0^{2,11}]undecane core that is constructed by an eight-, a three-, and a five-membered carbon ring. From a literature research, only one reference reported that a photoproduct featuring such a kind of bridged system was identified by IR, mass, and ¹H NMR spectroscopic methods.⁷ Herein, the X-ray diffraction analysis and quantum chemical calculation studies not only confirmed the novel carbon skeletons but also determined their absolute configurations. A biogenetic analysis (Scheme 1) obviously supports that 1–4 arise from preschisanartanin O (5), another new compound confirmed by NMR spectroscopic method (Tables S1 and S2, Supporting Information) and X-ray diffraction (CCDC 948231) (Figure 5). Intermediate A is derived from oxidation of 5 and further leads to the

(7) Dauben, W. G.; Kellogg, M. S. *J. Am. Chem. Soc.* **1972**, *94*, 8951–8953.

(8) Wirth, T. *Angew. Chem., Int. Ed.* **1996**, *35*, 61–63.

(9) Stromgaard, K.; Nakanishi, K. *Angew. Chem., Int. Ed.* **2004**, *43*, 1640–1658.

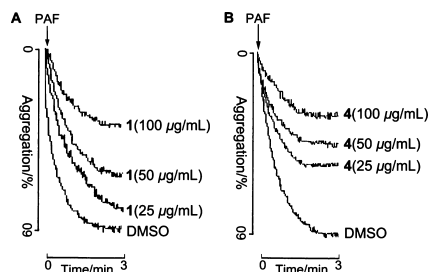


Figure 6. Compounds (A) 1 and (B) 4 inhibited platelet aggregation activity induced by PAF in a dose-dependent manner.

formation of a crucial carbon–carbon connection between C-12 and C-22 by a key pinacol coupling reaction.⁸

Ginkgolide B (GB), a specific platelet-activating factor (PAF) receptor antagonist, is a highly oxygenated diterpenoid containing a trilactone and tetrahydrofuran ring that are essential for the activity.⁹ Given that the structural characteristics of both the SNTs and GB are partially similar, compounds 1–5 were evaluated for their inhibition of platelet aggregation induced by PAF, collagen, arachidonic acid (AA), and thrombin. Our results showed that 1 and 4 specifically exhibited antiplatelet aggregation activity induced by PAF in a dose-dependent manner with IC₅₀ values of 79.95 and 52.26 μg/mL, respectively, but had no effect on that induced by collagen, AA, and thrombin (Table 1 and Figure 6). However, other isolates were either completely inactive or showed slight inhibition at 100 μg/mL (Table 1). Some research revealed that the IC₅₀ of GB was lower than 0.2 μg/mL in antiplatelet aggregation activity induced by PAF.^{9,10}

Acknowledgment. This project was supported financially by the NSFC (81373290), a CAS grant (KSCX2-EW-Q-10), the 973 programs (2009CB522300 and 2009CB930300), and the NSFYP (2012FB178) and sponsored by SRF for ROCS, SEM to W.-L.X. The calculation sections were supported by the HPC Center of Kunming Institute of Botany.

Supporting Information Available. Detailed experimental procedures, physical–chemical properties, 1D and 2D NMR, MS, IR, UV, and ECD spectra for compounds 1–5, and X-ray crystal structures (CIF) for compounds 1, 2, 4, and 5. This material is available free of charge via the Internet at <http://pubs.acs.org>.

(10) Hu, L. H.; Chen, Z. L.; Xie, Y. Y.; Jiang, Y. Y.; Zhen, H. W. *Bioorg. Med. Chem.* **2000**, *8*, 1515–1521.

The authors declare no competing financial interest.